

Determining Wave-Optics Mesh Parameters for Complex Optical Systems

Justin D. Mansell*, Robert Praus, and Steve Coy

MZA Associates Corporation, 2021 Girard Ste 150, Albuquerque, NM 87106

ABSTRACT

In prior work we introduced a method of choosing mesh parameters for a single wave-optics propagation between two effective apertures. Unfortunately, most systems that require wave-optics modeling, like modeling laser resonators with gain media, propagations through the atmosphere, and imaging systems with internal limiting apertures, have multiple apertures and phase screens that induce diffraction. We begin here by augmenting the single propagation theory to include diffraction from both apertures and phase aberrations. We then introduce a technique for analyzing complex systems of simple optics to determine the appropriate wave-optics mesh parameters.

Keywords: Fourier optics, wave-optics, mesh parameters, modeling, optical system modeling, mesh spacing, mesh size, complex systems.

1. INTRODUCTION

In this section the basics of wave-optics modeling are reviewed. Then a review of our prior work on choosing mesh parameters for a single propagation is provided as background.

1.1. Wave Optics Modeling

Wave-optics (a.k.a. Fourier optics) models simulate light using the Fresnel approximation of the Huygens-Fresnel principle.¹ Light propagated between two planes can be modeled using a two-dimensional Fourier transform of a grid of samples of the complex electric field. Although this technique is much more computationally intensive, it allows much more detail about the beam to be modeled including the effects of higher-order aberrations and the resulting system transfer functions like the modulation transfer function (MTF) or the optical transfer function (OTF).

Using the Huygens-Fresnel principle, the field amplitude, U , at a point in the output plane (x_2, y_2) is the superposition integral of points in the input plane, (x_1, y_1) , inside some limiting aperture Σ and the Green's function of free space (a.k.a. the propagation kernel), $h(x_1, y_1; x_2, y_2)$, which is written as,

$$U(x_2, y_2) = \iint_{\Sigma} h(x_2, y_2; x_1, y_1) U(x_1, y_1) dx_1 dy_1$$

where, in the case of relatively small angles,

$$h(x_0, y_0; x_1, y_1) = \frac{1}{j \cdot \lambda \cdot z} \exp(j \cdot k \cdot r_{12}),$$

$$r_{12} = \sqrt{(x_1 - x_2)^2 + (y_1 - y_2)^2},$$

and z is the axial distance between the input and output planes, λ is the wavelength of light being modeled, and k is the wave number ($2\pi/\lambda$). Using the Fresnel approximation, the kernel reduces to

$$h(x_1, y_1; x_2, y_2) = \frac{\exp(j \cdot k \cdot z)}{j \cdot \lambda \cdot z} \exp\left(j \frac{k}{2z} [(x_1 - x_2)^2 + (y_1 - y_2)^2]\right).$$

Using this form of the kernel, the propagation is a convolution of the input field with the kernel, and is referred to as the convolution propagator.

* jmansell@mza.com; phone 1 505 245-9970 x122

Further simplification allows the kernel to be decomposed into three separate terms which are two quadratic (or parabolic) phase terms in the input and output planes and a term that is directly analogous to the 2D Fourier transform operator. This form, referred to as the one-step propagator, is written as

$$U(x_2, y_2) = \frac{\exp(j \cdot k \cdot z)}{j \cdot k \cdot z} \exp\left(j \frac{kr_2^2}{2z}\right) \iint_{-\infty}^{\infty} \left\{ U(x_1, y_1) \exp\left(j \frac{kr_1^2}{2z}\right) \right\} \exp(-jkz(x_1x_2 + y_1y_2)) dx_1 dy_1$$

where

$$r_2 = \sqrt{x_2^2 + y_2^2} \quad \text{and} \quad r_1 = \sqrt{x_1^2 + y_1^2} .$$

This can be simplified into an operator notation as

$$U_2 = \frac{\exp(jkz)}{jkz} Q_2(z) \cdot F(U_1 \cdot Q_1(z))$$

where the $F(\dots)$ operator is the 2D Fourier transform operation and the $Q(z)$ is the quadratic phase factor with a radius of curvature of z , which can be written as

$$Q_x(z) = \exp\left(j \frac{kr_x^2}{2z}\right)$$

where the subscript, x , represents the plane of the operation.

1.2. Single Fourier Transform Modeling versus Double Fourier Transform Convolution Propagation Modeling

There are two commonly used ways of implementing Fourier transform modeling in a computer. The most basic wave-optics propagation modeling can be done with a single Fourier transform. Implementation of this form of propagator involves multiplying the field by the quadratic phase factor, Fourier transforming the field, and then multiplying by an additional quadratic phase factor and a scaling term. This is the fastest way of modeling optical propagation, but the mesh spacing in the output plane is related to the propagation distance, z , optical wavelength, λ , and the spacing in the input plane, δ_1 , by

$$\delta_2 = \frac{\lambda z}{\delta_1}$$

Because of the lack of control over the final plane mesh spacing in the one-step Fourier propagator, a convolution propagator is often used for wave-optics simulations. The convolution propagator is typically implemented on a computer by Fourier transforming the input field, multiplying by a convolution kernel, and inverse Fourier transforming the field. Implementation of this type of propagator is very convenient because unlike the one-step Fourier propagator, the input and output results are represented with the same grid spacing. The convolution propagator is generally performed relative to a planar reference so that the mesh spacing is the same, but in some cases, like propagating to the focal plane, a spherical reference wave is used to provide control over the target plane mesh spacing so that the field resolution can be controlled.

1.3. Numerical Modeling of the Optical Propagation

When doing numerical modeling of these continuous functions in a computer, the continuous functions are sampled onto a discrete mesh with a discrete number of mesh points and finite spacing between these points. Until recently, the existing literature on this topic is extremely vague on how to pick these mesh parameters. One of the best discussions of this topic is covered by Siegman.² He indicates that there is a need for the number of samples to be between 2 and 8 times the Fresnel number, N_f , which is defined as

$$N_f = \frac{r^2}{\lambda z},$$

where r is the radius of the aperture, λ is the wavelength, and z is the propagation distance. He also indicates that a guard-band of 2.4 to 3.0 times the aperture diameter is required to avoid beam spill-over.

Although these guidelines are a good start, there are times when they were not sufficient for addressing the problems that presented themselves. For example, if the Fresnel number of the propagation was 1/8, these guidelines indicated that only one point over the aperture was required to do the modeling. Another example is modeling a rapidly diverging or converging beam where the guard-band was insufficient. Even in the case of modeling propagation of a simple plane wave, a guard-band of 2.4 times the aperture diameter was excessive and resulted in unnecessary excessive computational time. The work here analyzes the mesh requirements based on the angular bandwidth required to represent the propagation relative to the Nyquist criteria and the periodic nature of the Fourier transform. In all the analysis done here, it is assumed that the field can be adequately represented on the predicted mesh or it can be filtered prior to the Fourier propagation to be so.

1.4. Choosing Mesh Parameters for a Single Propagation with Full-Aperture Illumination Theory

In prior work, we provided a technique for choosing mesh parameters that ensured that the mesh contained (1) enough angular bandwidth in phase space such that all the points in the input mesh could illuminate all the points in the output mesh (hence the full-aperture illumination theory name) and (2) enough guard-band so that Fourier wrap-around did not corrupt the region of interest in the target plane.³ We will review this analysis here for a case simplified by the limitation of 1D and the fact that the input and output regions of interest are the same diameter, D . Figure 1 shows a description of the effective problem geometry considered in light of periodic Fourier modeling. The first requirement of simple Fourier modeling is to model sufficient angular bandwidth so that light traveling from one side of the input region of interest can illuminate the opposite side of the output region of interest. The complex number representation of an electric field wraps the phase such that it is only between $-\pi$ and π , thus creating an effective oscillation in the phase. Nyquist sampling requires that at least two samples of the phase are taken for each 2π phase oscillation. A 2π radian phase step is equivalent to a one wavelength, λ , step height. Thus, the Nyquist requirement can be represented mathematically as

$$\theta = \frac{D}{z} \Rightarrow \frac{\lambda}{2\delta} \geq \frac{D}{z} \Rightarrow \delta \leq \frac{\lambda z}{2D}$$

where δ is the spacing between samples.

The next requirement comes from the fact that the discrete Fourier transform assumes a periodic input. To illustrate this, Figure 1 shows effective apertures adjacent to the input aperture and shows the effect of light diverging from their edges impinging on the adjacent mesh. If the region of interest in the output plane is limited to a diameter D , accuracy in the area outside this diameter can be sacrificed by allowing the effective adjacent apertures to illuminate this area in order to reduce the number of required mesh points to speed up the modeling. Thus, the mesh diameter, D_{mesh} , can be represented by

$$D_{mesh} = D + \theta z = D + \frac{\lambda z}{2\delta}$$

The required number of mesh points is then the ratio of the mesh diameter to the mesh spacing, or

$$N \geq \frac{D_{mesh}}{\delta} = \frac{4D^2}{\lambda z} = 16 \cdot \frac{r^2}{\lambda z} = 16 \cdot N_f$$

where N_f is the Fresnel number.

This analysis was extended for non-equal sized input and output regions of interest so that spherical wave propagation could be addressed.³ The resulting inequalities are given by

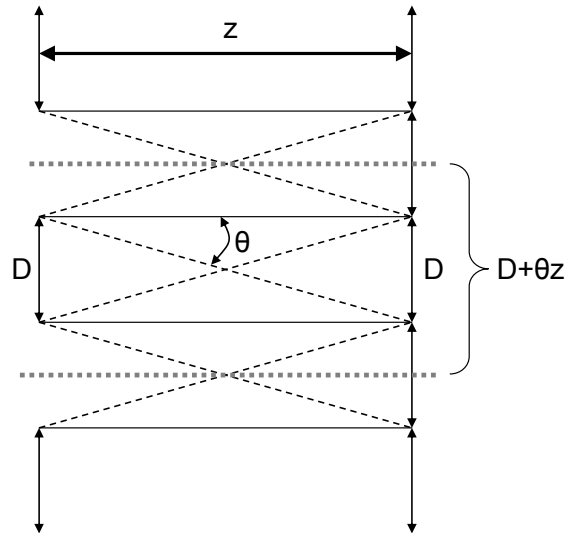


Figure 1 - Variable definition for choosing mesh parameters for a simple propagation

$$\delta_1 D_2 + \delta_2 D_1 \leq \lambda z$$

$$N \geq \frac{D_1}{\delta_1} + \frac{D_2}{\delta_2}$$

where δ_1 is the mesh spacing in the input plane, D_2 is the diameter of the region of interest in the output plane, δ_2 is the mesh spacing in the output plane, and D_1 is the diameter of the region of interest in the input plane.

For a given propagation, the mesh parameters that minimize the number of mesh points, and hence the computational difficulty of the problem, are given by

$$\delta_1 = \frac{\lambda z}{2D_2}, \quad \delta_2 = \frac{\lambda z}{2D_1}, \quad N \geq \frac{4D_1 D_2}{\lambda z}.$$

These mesh parameters have direct optical significance. Each of the mesh spacings are equivalent to the half the diffraction limited spot radius of a square aperture viewed from the opposite aperture. In the case of equal sized starting and ending regions of interest ($D_1 = D_2$), the number of mesh points should be larger than 16 times the Fresnel number. For unequal aperture sizes, the number of mesh points is equal to 16 times the collimation Fresnel number, which is defined by Siegman as⁴

$$N_c \equiv \frac{D_1 D_2}{4z\lambda} = \frac{MD_1^2}{4z\lambda},$$

where M is the effective magnification, which is defined as D_2/D_1 .

1.5. Modeling Added Angular Bandwidth from Kolmogorov Turbulence

In prior work, Coy outlined a procedure for adding the angular bandwidth from Kolmogorov turbulence.³ Turbulence can be reduced to an effective turbule size in the input aperture, r_0 . The angular spreading induced by the turbulence can be approximated by

$$\theta_{urb} = \gamma \frac{\lambda}{r_0}$$

where γ is a turbulence scaling factor. Coy adjusts the effective diameter of the region of interest by adding the angular content induced by the turbulence as

$$D' = D + \gamma \frac{\lambda z}{r_0}.$$

The full-aperture illumination inequalities were then used to find the mesh parameters based on the new diameter of the region of interest. Coy also presents guidelines for choosing γ based on the amount of energy the model wants to represent based on a Kolmogorov phase screen. The result of this analysis was that more than 90% of the energy could be represented for a value of γ of 3.

The added angular bandwidth of a turbulence phase screen is directly analogous to the diffraction angle of a grating, which is represented mathematically as,

$$\sin(\theta) = N \frac{\lambda}{\Lambda}$$

where N is the diffractive order and Λ is the grating period. In the small angle approximation, $\sin(\theta) \approx \theta$. Since this theory provides a mechanism of taking phase screens into account, we will refer to this modification to the full-aperture illumination theory as the phase diffraction theory.

2. THE DIFFRACTION THEORY OF MESH PARAMETER DETERMINATION

An alternative method of determining the angular content of a beam is to use the diffraction angle from the edges of the aperture. For a given hard-edge aperture, diffraction predicts spreading of the light by an angle proportional to the ratio of wavelength to the aperture diameter (λ/D). If we use a proportionality factor of η , we can derive a reduced set of mesh parameters for a case of equal sized input and output regions of interest as

$$\frac{\lambda}{2\delta} \geq \eta \frac{\lambda}{D} \Rightarrow \delta \leq \frac{D}{2\eta}$$

$$N \geq \frac{D}{\delta} + \frac{\lambda z}{2\delta^2}$$

These inequalities predict a set of mesh parameters based on edge diffraction, so we will label this technique the edge-diffraction theory. When η is equal to the 4 times the Fresnel number ($D_2/\lambda z$), these edge-diffraction mesh parameters are equal to the full-aperture illumination parameters derived above. Practical values for η can be estimated by analyzing the energy capture with respect to angle for common diffraction patterns. The normalized diffraction patterns from a Gaussian, a circular aperture (Airy pattern), and from a square aperture (sinc pattern) were integrated after applying a 10^{-10} threshold. Figure 2 shows the results of this analysis. A good value for η for most applications is 5 because for all the common diffraction patterns the majority of the energy is being represented.

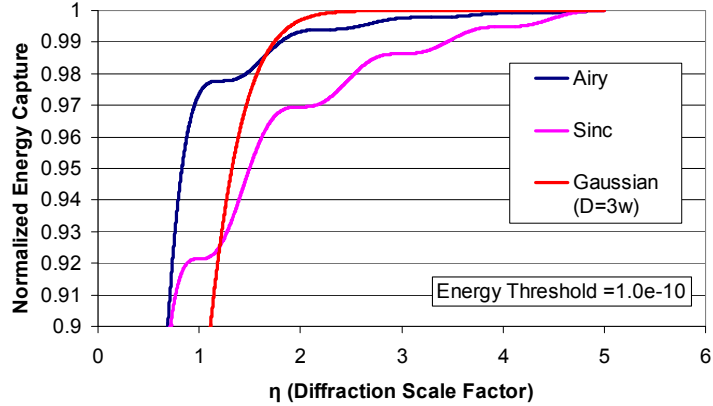


Figure 2 - Normalized energy capture for varying values of the diffraction scale factor

diffraction patterns from a Gaussian, a circular aperture (Airy pattern), and from a square aperture (sinc pattern) were integrated after applying a 10^{-10} threshold. Figure 2 shows the results of this analysis. A good value for η for most applications is 5 because for all the common diffraction patterns the majority of the energy is being represented.

There are two cases in which the full-aperture illumination theory of determining mesh parameters can provide difficulties: large Fresnel number propagation and small Fresnel number propagation.

2.1. Large Fresnel Number Propagation Modeling

The above inequalities ensure that the mesh is properly represented for a single propagation, but these requirements can be conservative for large Fresnel number propagation (short distances and/or large apertures). Often, for large Fresnel number propagations, the inequalities given above require a mesh that is outside practical limitations like computer memory. The edge-diffraction theory above can be used to predict a reduced set of mesh points that are adequate, especially if the large Fresnel number propagation is followed by a lower Fresnel number propagation, as is the case for modeling the internal and external propagations of a directed energy system.

Changing the z term in the inequality for N from the short distance to a total system distance allows us to obtain accurate answers in later planes. As an example, we analyzed a system with a 1.0-m diameter aperture propagating a distance of 1 km with a wavelength of $1.0 \mu\text{m}$ before propagating a distance of 250 km. This is equivalent to the initial short propagation of a 10-cm diameter beam being propagated 10 m before being expanded in a 10x telescope to be propagated to a far-off target. Using the inequalities that take into account the full angular extent, the required mesh (on a power of 2 number of mesh points) has 4096 points with a spacing of $500 \mu\text{m}$. Using the reduced angular bandwidth with $\eta=15$ required only 1024 mesh points (again on a power of 2) with a 33 mm mesh spacing. Results of the field amplitudes at the intermediate and final planes are shown in Figure 3.

The field pattern at the intermediate plane for the reduced mesh is clearly not sufficiently resolved to see the Fresnel ringing, but clearly produces a much superior result at the final plane. In this intermediate plane, we are only modeling a portion of the light, but in the final plane the portion of light that is modeled fills the entire region of interest. The full resolution result looks good at the intermediate plane, but has suffered from a great deal of wrap-around at the final plane.

This technique of using reduced angular content based on diffraction is a good way of reducing a complex problem that might not otherwise be able to be modeled with wave-optics due to the large number of required mesh points and producing an answer that is not fully accurate, but often has acceptable accuracy for real-world problems.

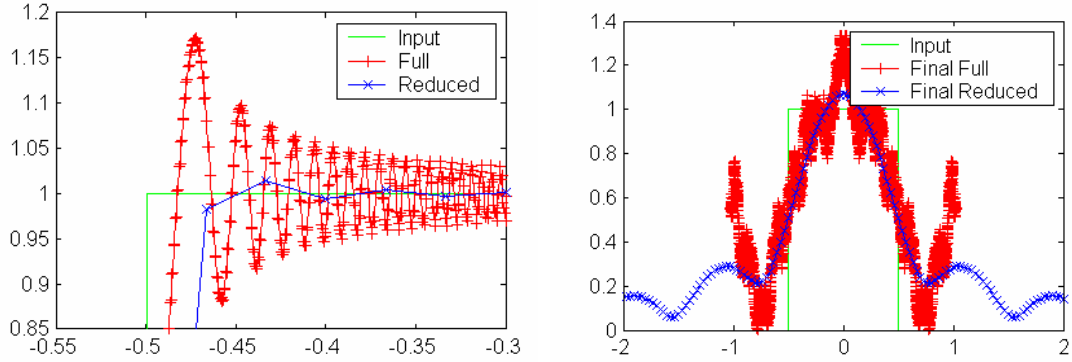


Figure 3 - Results at the intermediate and final planes of the full mesh and the reduced mesh.

2.2. Small Fresnel Number Propagation Modeling

Another case that is difficult to model using the minimum mesh parameters predicted by the full-aperture illumination theory is the case of long propagations or small Fresnel numbers. As an example, consider propagation of 1.0 μm light from a 20 mm aperture over a distance of 100 m. We modified the theory so that the mesh spacing (dx) was smaller than the inequality required in each case, but was set to an exact odd integer multiple of the aperture diameter. Thus, the full-aperture illumination theory predicts a minimum mesh of 32 points and a spacing of 2.2 mm, which allows exactly 9 samples across the diameter of the region of interest. The edge-diffraction theory with $\eta=10$ predicted a mesh with 128 points and a mesh spacing of 0.952 mm, which corresponds to 21 samples of the field across the diameter of the region of interest. Figure 4 shows the results of this Fourier modeling with the results of the numerical integration of the analytical form of the Fresnel integral for a slit on a 512 sample grid with a spacing of 0.156 mm. The Fresnel integral solution for a slit can be represented as²

$$u(y) = \sqrt{jN_f} \int_{-1}^1 \exp(-j \cdot \pi \cdot N_f \cdot (y - y_0)^2) dy_0$$

where u is the field, y is the normalized lateral dimension coordinate ($y=x/a$), a is radius of the slit, and N_f is the Fresnel number. This integral was integrated simply by summing 10^4 discrete evaluations of the function over the -1 to +1 range.

The theoretical answer was compared to the results obtained for varying values of η in two ways. The first error term was calculated by taking the difference in on-axis intensity between the Fourier modeling result and the theoretical result and was normalized by the theoretical on-axis intensity value. The next error was calculated by taking the rms difference between the theoretical field

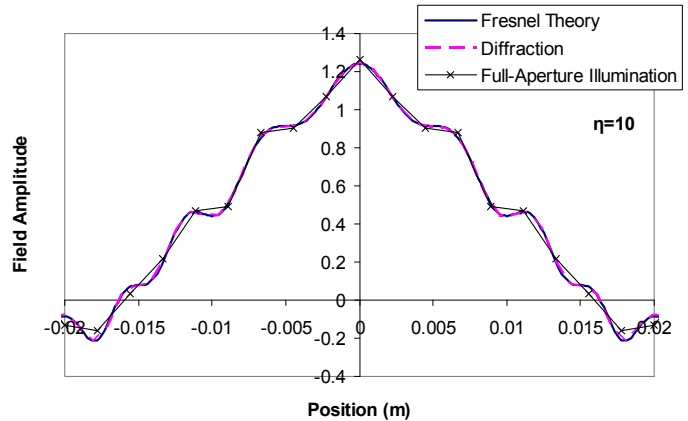


Figure 4 - Results of the 1D propagation modeling of a slit with a Fresnel number of 1.0 compared to the Fresnel integral theory.

interpolated on to the same grid as the Fourier result and the Fourier result evaluated over the output region of interest. The output region of interest in this case had the same diameter as the input region of interest, which equaled 20 mm. Then this error was normalized by dividing by the peak intensity of the theoretical result to create a coefficient of variance. Figure 5 shows these two error terms with respect to varying values of the diffraction scaling factor, η . The point with the lowest diffraction scaling factor is the result predicted by the full-aperture illumination theory. The next

point is the result for the $\eta=10$ case, which showed an on-axis intensity error of 5.9% and a intensity coefficient of variance of 0.4%.

In conclusion, the diffraction theory of choosing mesh parameters offers the modeler an alternative to the full-aperture illumination theory that is especially useful in the case of very short or very long propagations. In the next section we present a theory that unites the three theories presented above.

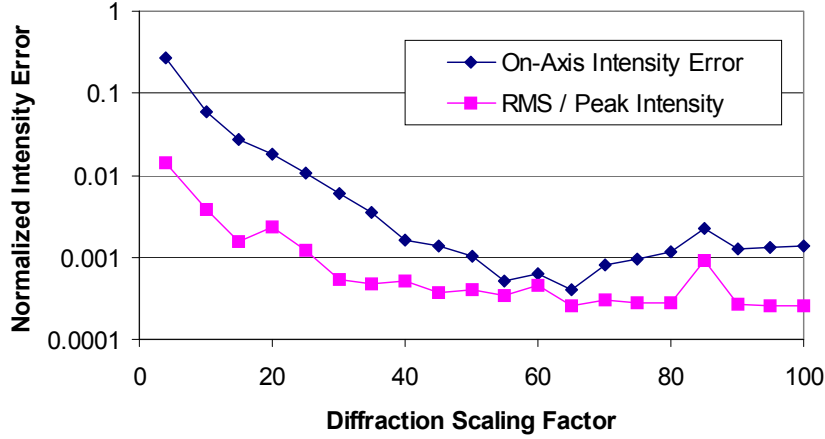


Figure 5 - Two forms of intensity error with respect to the diffraction scaling factor comparing Fourier modeling to the theoretical value based on a high-resolution evaluation of the Fresnel integral result for a slit with a Fresnel number equal to 1.0

3. COMBINING THE MESH PARAMETER DETERMINATION THEORIES

We have presented three variations of the theory on how to determine mesh parameters in this paper: the full-aperture illumination theory, the phase diffraction theory, and the edge diffraction theory. The most conservative technique of combining all of these different theories is to add their components of angular bandwidth such that the total modeled angular bandwidth for an equal aperture system with equal effective r_0 values on each end is given by

$$\theta = \frac{z}{D} + \eta \frac{\lambda}{D} + \gamma \frac{\lambda}{r_0}.$$

For a system with unequal apertures, the total angular bandwidth is

$$\theta = \frac{D_2 + D_1 \cdot \delta_2 / \delta_1}{2z} + \eta \frac{\lambda}{D_{\min}} + \gamma \frac{\lambda}{r_0}$$

From this angular bandwidth, we can determine the required mesh spacing based on Nyquist sampling to be

$$\frac{\lambda}{2\delta} \geq \theta \Rightarrow \delta \leq \frac{\lambda}{2\theta}.$$

Then the number of mesh points required to avoid the periodic wrap-around effects of Fourier modeling is

$$N \geq \frac{D_2 + \theta \cdot z}{\delta}.$$

These two inequalities provide a conservative but fairly complete theory taking into account phase-induced diffraction, edge-induced diffraction, and the full-aperture illumination requirements of Fourier modeling. The degree to which the phase and edge diffraction is represented is adjustable by the user via the η and γ coefficients.

4. COMPLEX SYSTEM MODELING

In the work above, the analysis was limited to a single propagation between two regions of interest, but modeling a complex system typically requires multiple propagations. The analysis above showed that the required mesh parameters can be determined given a wavelength and two regions of interest separated by a distance. Therefore, we present here a procedure for reducing a complex system to two limiting apertures and a single distance for determining the mesh parameter requirements based on field and aperture stop analysis.

4.1. Field and Aperture Stop Determination

In every optical system there is both an aperture stop, which limits the cone of energy from a point on the optical axis, and a field stop, which limits the angular extent of the light going through the system.⁵ Born and Wolf outline a procedure to find the aperture stop and field stop of a complex optical system comprised of simple optical elements as follows:⁶

1. Find the location and size of the image of each of the apertures in the input space. This can be done using the imaging equation⁷, $1/f = 1/d_1 + 1/d_2$, or through any comparable means.
2. Find the angle formed by the edges of each of the apertures and a point in the middle of the object being imaged.
3. The aperture which creates the smallest angle is the image of the aperture stop, or the entrance pupil.
4. Find the angle formed by a point in the center of the entrance pupil and the image of each of the other apertures.
5. The aperture which creates the smallest angle is the image of the field stop.

The field stop and aperture stop are the apertures in an optical system that most limit the cone angle of light entering the system and the field of view of the system. For a given optical system, the image of these two apertures in the input space and the separation of their images is all the information needed to determine the mesh for modeling a complex optical system comprised of simple optical elements. We modified this procedure slightly to address the wave-optics modeling problem by replacing the object with the light source and its aperture. We also found that using ABCD ray matrices⁸ was a convenient way of determining the image planes of the various apertures in the system. To determine the size and location of the image of a given aperture, the ABCD matrix representing the propagation from the source to the aperture was inverted and the resulting inverted ABCD matrix revealed the effective magnification, M_{image} , and image plane location, z_{image} , by

$$\begin{bmatrix} 1 & z_{image} \\ 0 & 1 \end{bmatrix} \cdot \begin{bmatrix} A & B \\ C & D \end{bmatrix}_{inverted} = \begin{bmatrix} M & 0 \\ C & 1/M \end{bmatrix}$$

$$z_{image} = -B/D$$

$$M_{image} = C \cdot z_{image} + A$$

4.2. Imaging System Example

Figure 6 (a) shows a complex imaging system comprised of ideal simple optical elements. Figure 6 (b) shows the simplified system in which the apertures have been imaged back into the input plane. The lens L1 forms the aperture stop and the input aperture, A1, forms the field stop. The images of the two apertures in the input space are 15 mm and 1 mm in diameter respectively. They are separated by a distance of 15 mm. For a wavelength of 1.0 μm , the resulting mesh parameters for the system with $\gamma=0$ and $\eta=0$ are 512 x 9.4 μm .

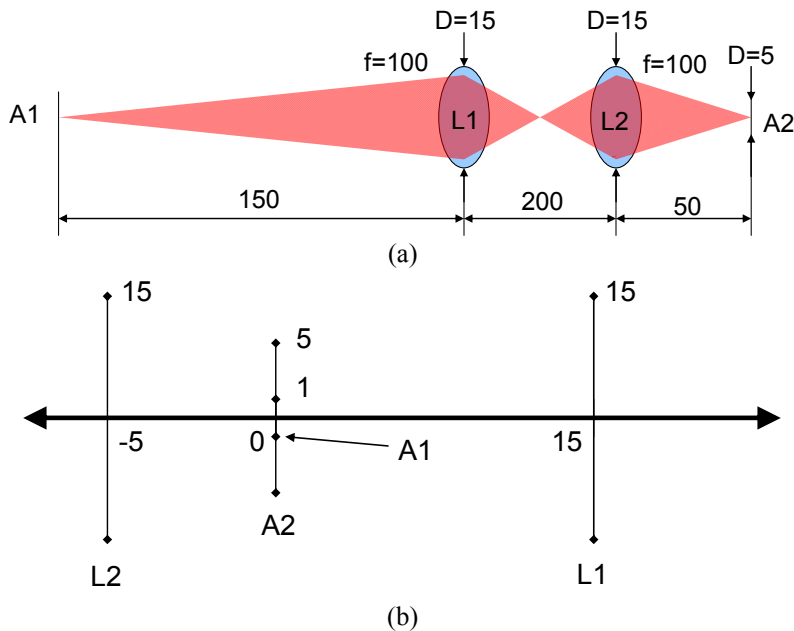


Figure 6 - An imaging system (a) and its resulting input-plane aperture representation (b)

Figure 7 shows the field magnitude results of modeling a uniform plane wave entering the system using these mesh parameters with a spherical reference wave modified directly by the lenses. Plane 1 is the input plane after the 1-mm input aperture. Plane 2 is the plane of the first lens, L1. Plane 3 is the plane of the second lens, L2. Plane 4 is the image plane. It is clear from this result that the image is very good because it lies exactly on top of the input.

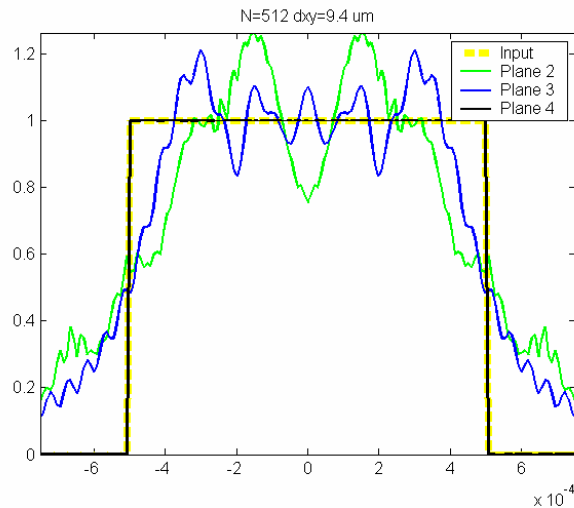


Figure 7 - Results from sequential spherical reference wave wave-optics modeling of the imaging system

To show the effects of diffraction, the system was modeled again with the input aperture reduced in size to 0.1 mm in diameter. With the diffraction scale factor, $\eta=0$, the mesh parameters were $4096 \times 9.9 \mu\text{m}$. The results of the propagation to the same planes as the example above are shown in Figure 8. One key learning from modeling this

system is that the 15 mm aperture lenses clip some of the diffraction from the small input aperture. This is partially shown in the image plane (Plane 4) as a slight ripple, but it is under-resolved.

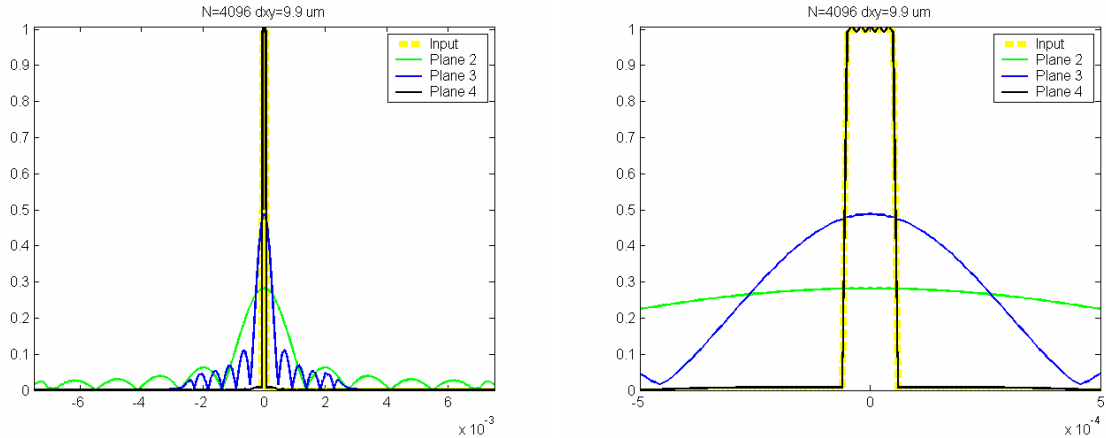


Figure 8 - Sequential wave-optics modeling results using a 100-micron input aperture

To get better resolution on the ripple on the far-field pattern, the diffraction scale factor, η , was increased to 5. The resulting mesh parameters for this model were then $8196 \times 5.0 \mu\text{m}$. Figure 9 shows the results of this modeling. The diffraction ripple in the image plane (Plane 4) is much more clearly resolved indicating a more accurate model of the system. The disadvantage of this more-accurate model was the increase in computational difficulty.

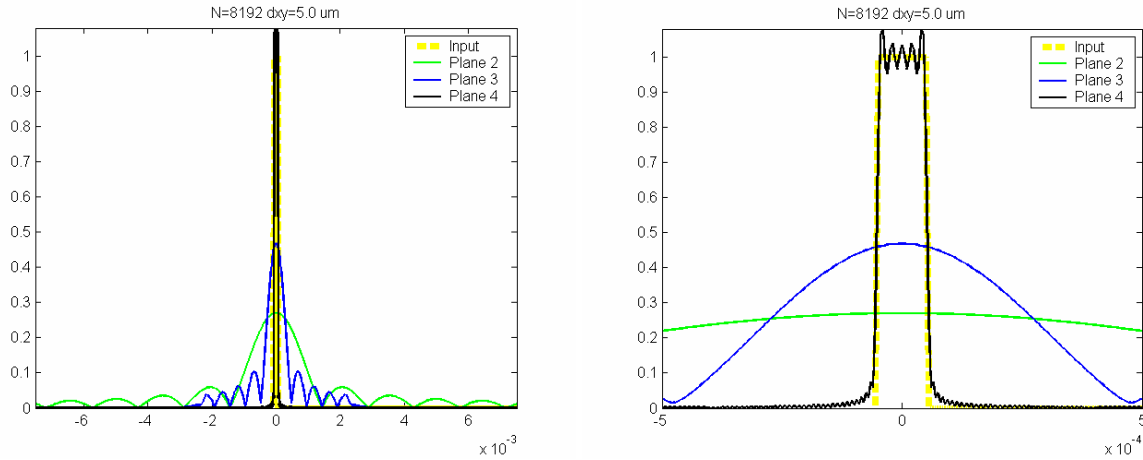


Figure 9 - Wave-optics results of modeling the imaging system with a 0.1-mm input aperture and a diffraction scale factor of 5.0

5. CONCLUSIONS

We present here a series of common problems when modeling complex systems with wave-optics, including large and small Fresnel number propagation, systems with a series of apertures, and systems with turbulent phase screens. The results allow a user sufficient flexibility when modeling a complex optical system so as to be able to represent the propagation correctly in every wave-optics model.

Acknowledgements

This work was funded under contract to the ABL SPO. We offer our thanks to Dr. Salvatore Cusumono and Captain Jason Tellez for their continued contributions and support.

REFERENCES

-
- ¹ J. Goodman, *Introduction to Fourier Optics*, Ch. 3-4, McGraw-Hill, New York, 1988.
 - ² A. E. Siegman, *Lasers*, Ch. 18, University Science Books, Mill Valley, CA, 1986.
 - ³ S. Coy, "Choosing mesh spacings and mesh dimensions for wave optics simulation", SPIE Vol. 5894, 45-56, 2005.
 - ⁴ A. E. Siegman, *Lasers*, Ch. 20, University Science Books, Mill Valley, CA, 1986.
 - ⁵ W. J. Smith, *Modern Optical Engineering*, 3rd Ed., McGraw-Hill, New York, 2000.
 - ⁶ M. Born and E. Wolf, *Principles of Optics*, 7th Ed., Ch. 4, Cambridge University Press, Cambridge, UK, 1999.
 - ⁷ B. A. E. Saleh and M. C. Teich, *Fundamentals of Photonics*, Ch. 1, Wiley, New York, 1991.
 - ⁸ A. E. Siegman, *Lasers*, Ch. 15, University Science Books, Mill Valley, CA, 1986.